Electronic Supplementary Material (ESI) for Lab on a Chip.


# Supporting information for:

# *A microfluidic platform with pH imaging for chemical and hydrodynamic stimulation of intact oral biofilms*

M. Parvinzadeh Gashti,[ad] J. Asselin,[abd] J. Barbeau,[c] D. Boudreau,[ab] J. Greener[a]*

Department of Chemistry[a] and Centre d'optique, photonique et laser (COPL),[b]

Université Laval, Québec (QC) Canada G1V 0A6

Faculté de médecine dentaire, Université de Montréal (QC), Canada H3C 3J4,[c]

* Corresponding author: *jesse.greener@chm.ulaval.ca*

[d] Co-first authors

## MATERIALS AND METHODS

***Chemical and reagents.*** Sodium citrate tribasic dihydrate (≥99.0% ACS grade), sodium borohydride (99.99%), fluorescein 5(6)-isothiocyanate (FiTC; 90%), triethylamine (≥99.5%), (3-aminopropyl)triethoxysilane (APTES; ≥98%), dimethylamine (40 wt% solution in water), and L-ascorbic acid (HAsc; ≥99.0%) were purchased from Sigma-Aldrich. Silver nitrate (99.9995%) was obtained from Strem Chemicals, (TEOS; 99.9%) from Alfa Aesar, and anhydrous *N*,*N*-dimethylformamide (DMF; 99.8%) from EMD Chemicals, *O*-(propargyloxy)-*N*-(triethoxysilylpropyl)-carbamate (PTSC; 90%) was purchased from Gelest, 11-azidoundecyltrimethoxysilane (AUTS; ≥95%) from SiKÉMIA, copper sulfate pentahydrate (≥98.5%) from VWR International. Buffers were prepared with potassium phosphate monobasic (≥99.0%, Anachemia) and precise volumes of sodium hydroxide (97.0% ACS, BDH) aqueous solution. Unless otherwise specified, every chemical reagent was used without further purification. Ultrapure water (18.2 MΩ) was used in all experiments unless specified and anhydrous ethanol, obtained from Commercial Alcohols, was used as a solvent. All glassware for nanoparticles synthesis was conditioned with concentrated nitric acid, and then rinsed thoroughly with water.

***Nanoparticle synthesis and surface attachment.*** The procedure to prepare silver cores follows a seed-growth reduction methodology derived from various works cited in literature.[1-3] Small silver seeds were synthesized to be used as nucleation points in growth reactions. In a 250 mL round bottom flask, 75 mL of ultrapure water was vigorously stirred, heated to 70°C before addition of 20 mL of 1 wt% sodium citrate in water (34 mM). After 10 minutes to allow stabilization of the temperature in solution, 1.7 mL of 1 wt% $AgNO_3$ (59 mM, purity 99.0%) and 0.2 mL of freshly-made 1 wt% $NaBH_4$ (264 mM) were added quickly. The mixture is left under agitation for 30 minutes before cooling to ambient temperature; colloids were kept overnight in the dark at 4°C to allow deactivation of residual borohydride moieties in the aqueous solution. Afterward, the diameter of these seeds was increased in three successive steps. First, 75 mL of nanopure water and 2.0 mL of fresh 1 wt% citrate solution were put to a boil in a $HNO_3$-cleaned 250

mL single-neck round bottom flask equipped with a reflux and immersed in a 120°C oil bath under vigorous stirring. Additions of 15.0 mL of seeds and 1.7 mL of fresh 1 wt% $AgNO_3$ were made with a 30-second delay in-between. After 1h of reaction and cooling for 30 minutes, uniform 20-nm Ag NPs were obtained and diluted to 100 mL. Second, 75 mL of nanopure water and 12.5 mL of the previous colloids were stirred to 88 °C in a clean 250 mL round bottom flask before successive additions of 2.0 mL 1 wt% sodium citrate and 1.7 mL 1 wt% silver nitrate, with 30 seconds delay in-between. The mixture was left to react for 2 hours before cooling to ambient temperature under moderate stirring and further dilution to 100 mL. Third, 30 mL of these 45-nm NPs was diluted in 60 mL of nanopure water to prepare the final 80-nm cores. Suspensions were stirred to 85 °C before addition of 2.0 mL 1 wt% sodium citrate and 1.7 mL 1 wt% $AgNO_3$, again with 30 seconds-between. All dispersions were diluted to 100 mL and kept in the dark at 4°C.

The condensation of a silica shell on the silver core was achieved using experimental conditions adapted from Blaaderen et *al*.[4] A fluorescent silane precursor was prepared from the pH-sensitive fluorophore molecule, a step adapted from our previous works.[5-8] Typically, 2.2 mg of FiTC was added to 114 µL of DMF, 1.6 µL of triethylamine and 1.6 µL of APTES, and left to agitate for 2h – thus obtaining a 50 mM solution of the desired molecule. This mixture was then diluted to a volume of 13.5 mL with anhydrous ethanol. A 100 mL volume of the suspension of 80-nm Ag nanoparticles was diluted in 600 mL of ethanol, and 14 mL of 10 mM TEOS/EtOH and 8 mL of dimethylamine were added in order to form a thin silica layer. After 15 minutes, a new addition of 4.4 mL of the FiTC-APS precursor solution previously described was added and left to react for 20-24h at room temperature, and the resulting suspensions were washed in ethanol and centrifuged three times (8,000 RCF, 15 minutes). Grafting of the core@shell $Ag@SiO_2$+FiTC NPs was done following a method developed in our previous work.[9] The surface activation of 24×30 mm silica coverslips was obtained by immersion in Piranha 3 $H_2SO_4$ : 1 $H_2O_2$ (30%) for 45 minutes. After thorough rinsing with water and conditioning in ethanol, two substrates were deposited in

each of the polypropylene Petri 100×100 mm dishes and put in contact with 2 mM of AUTS/EtOH solution under moderate agitation for 3 hours. Following the reaction, they were rinsed and stored overnight in water to complete the hydrolysis of the silane moieties. Functionalization of Ag@$SiO_2$+FiTC nanoparticles with the coupling agent was done in 4 mM PTSC/EtOH for 4 hours, before being purified by centrifugation (8 000 RCF, 15 minutes) and dispersed in ethanol. In a Petri dish, 5 mL of core-shell particle suspension, 1.5 mL of freshly prepared 5 mM copper sulfate solution, and 1.5 mL of 5 mM ascorbic acid in 66% ethanol-water solution were mixed and left to react under agitation for various durations and then rinsed several times in ethanol and water in a sonication bath.

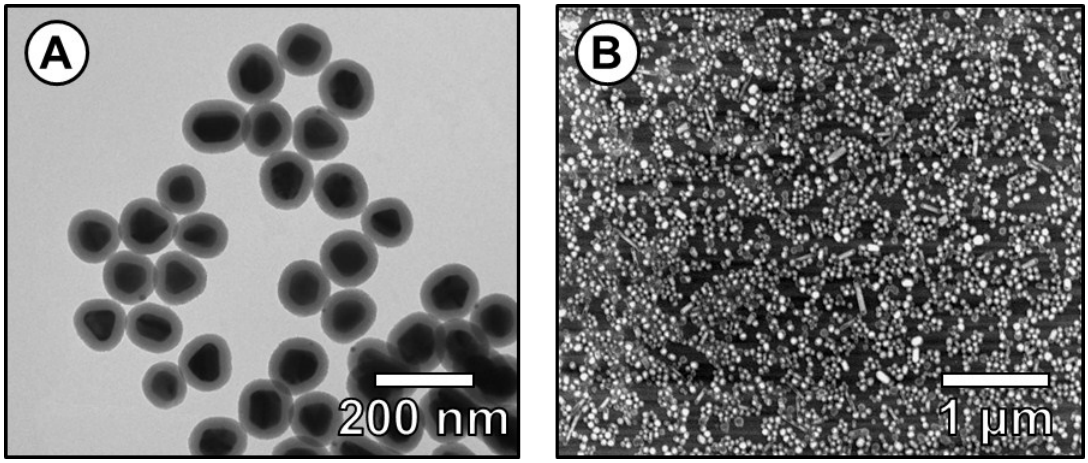


**Figure S1.** A) Transmission electronic micrograph of Ag@$SiO_2$+FiTC NPs with dimensions of (80±10) nm for the core and (15±1) nm for the silica shell. B) Scanning electron micrograph of Ag@$SiO_2$+FiTC NPs grafted on a glass coverslip.

***Native pH responsivity of as-prepared nanoparticles.***

The response of grafted Ag@$SiO_2$+FiTC NPs to pH variations was evaluated before the preparation of microfluidic channels by submersion in 0.100 M phosphate buffers and thorough rinsing between each samples. $FC_1$ and $FC_3$ filter combinations were used to apply the ratiometry normalization. Instrumental parameters are described in the main text.

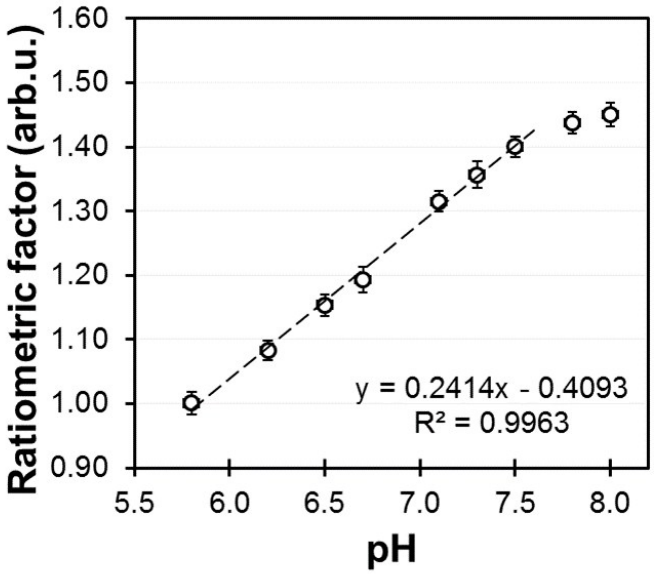


**Figure S2.** Ratiometric calibration curve measured for Ag@$SiO_2$+FiTC-NPs surface and filter combinations $FC_1/FC_3$.

***Instrumentation.*** Nanoparticle suspensions were analysed by UV-visible spectrophotometry (Cary 50), transmission electronic microscopy (Tecnai G2 Spirit Biotwin), and scanning electron microscopy (Quanta 3D, FEI). Characterization of the functionalised and grafted surfaces was achieved by UV-visible spectroscopy and spectrofluorimetry (Jobin Yvon Fluorolog 3-22 equipped with a cooled PMT R928 detector, Horiba).

***Fluid delivery.*** Liquid was delivered to the microfluidic device using connective tubes from perfluoroalkoxy (PFA) with outer diameter 1.6 mm (U-1148, IDEX, WA, USA), which were connected to polypropylene syringes (BD Scientific, NJ, USA) using connector assemblies (P-200x, P-658, IDEX, USA). Buffer solutions were fed into the microfluidic devices using a syringe pump (PHD 2000, Harvard Apparatus, USA).

***Resistance to photobleaching.*** As discussed in the main paper, we undertook photobleaching experiments to demonstrate that a stable intensity can be reached after uniform exposure for a certain period of time. In this case, we flowed a pH 7.0 buffer at $Q$=0.05 mL/s and used a 10x objective to illuminate an area

measuring 454 μm×340 μm area for 2 hours using the $FC_2$ filter combination (description in main text). As seen in Figure S3, the intensity diminishes exponentially until reaching a steady state after approximately 45 min. The calibration curves obtained before and after the photobleaching (Figure S4) are different. We note that, while the sensitivity goes down after photobleaching, benefits include a wider linear range and a stability over long-duration experiments.

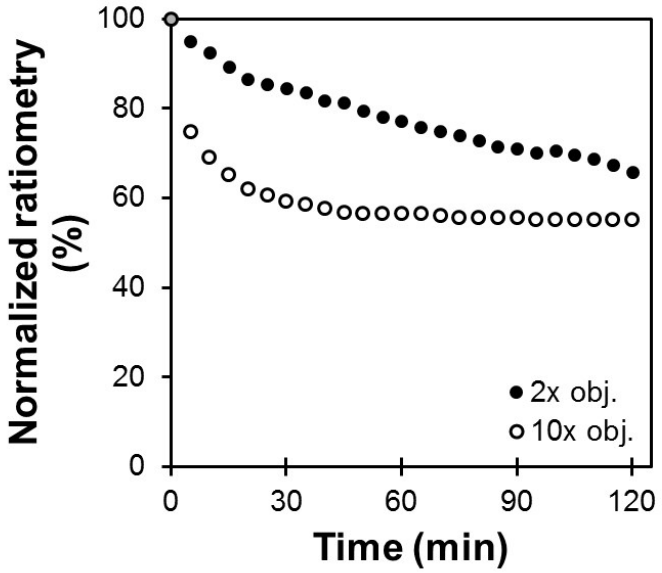


**Figure S3.** Reduction in fluorescence emission intensity ratios of the nanoparticle sensing layer ($FC_1/FC_3$) at intervals between continuous exposure using filter combination $FC_2$ and 2x and 10x objectives.

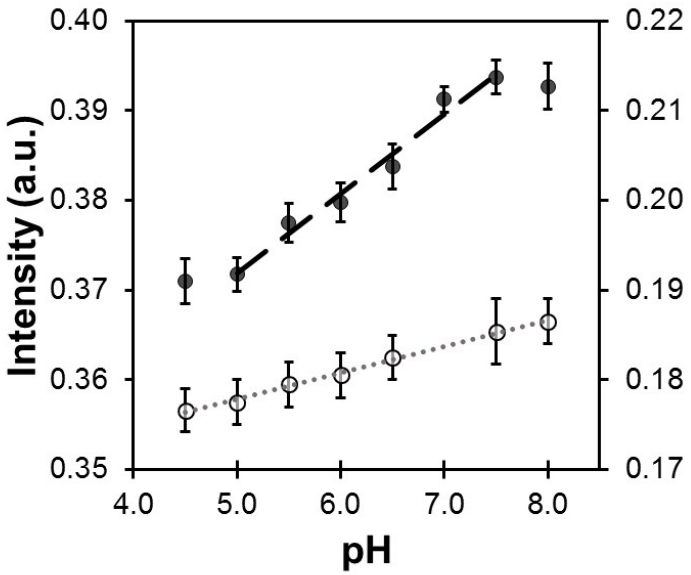


**Figure S4.** A) Calibration curve of $Ag@SiO_2$+FiTC surfaces before (solid circles, left axis, $y$=0.0089x+0.3275) and after (open circles, right axis, $y$=0.0015x+0.1773) photobleaching with 10x objective and $FC_2$.

***Biofilm formation in microchannels.*** Acidic *Streptococcus salivarius* bacterial biofilms were grown in one arm of a Y-junction device, using LB growth medium containing 0.1 wt% NaCl, 0.1 wt% Tryptone and 0.05 wt% yeast extract. Here we present the two separate images used to generate Figure 5C in the main paper. Figure S5A shows the ratiometric image with the parts in green representing those locations where the pH is lower than the background. This image was generated by inverting pixel intensity and adjusting the brightness/contrast to show only the most acidic portions of the field of view. The acidic portions overlap with the thick portions of the biofilm shown in Figure S5B as the optically dense biofilm from the transmission-mode image.

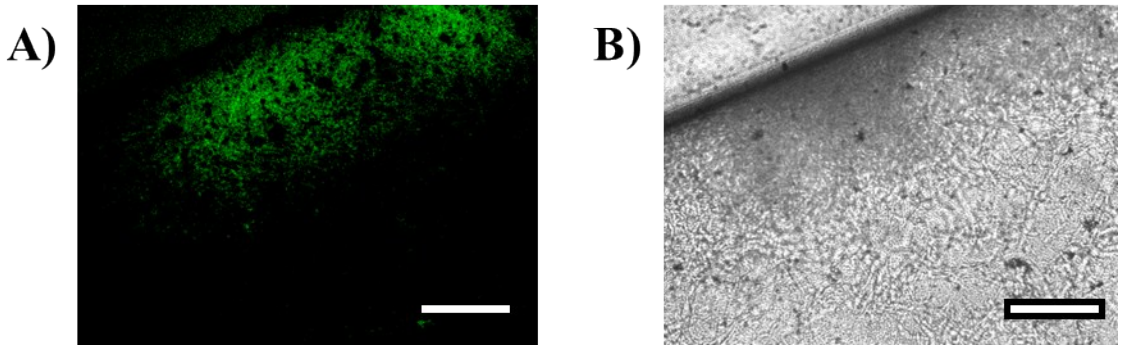


**Figure S5.** A) False coloured representation of a ratiometric pH image of a locally dense portion of *Streptococcus salivarius* bacterial biofilm. B) Transmission image of the same region in A). Both A and B were acquired using a 10x objective. Scale bars in A and B are 100 μm.

## REFERENCES


1. Li, H.; Xia, H.; Wang, D.; Tao, X. *Langmuir*, **2013**, 29, 5074-5079.
2. Wan, Y.; Guo, Z.; Jiang, X.; Fang, K.; Lu, X.; Zhang, Y.; Gu, N. *J. Colloid Interface Sci.*, **2013**, 394, 263-268.
3. Bastús, N. G.; Merkoçi, F.; Piella, J.; Puntes, V. *Chem. Mater.*, **2014**, 26, 2836-2846.
4. Tovmchenko, O. G.; Graf, C.; Van den Heuvel, D. J.; Van Blaaderen, A.; Gerritsen, H. C. *Adv. Mater.* **2006**, 18, 91-95.
5. Viger, M. L.; Live, L. S.; Therrien, O. D.; Boudreau, D. *Plasmonics*, **2008**, 3, 33-40.
6. Rainville, L.; Dorais, M.-C.; Boudreau, D. *RSC Adv.*, **2013**, 3, 13953-13960.
7. Brouard, D.; Ratelle, O.; Bracamonte, A. G.; St-Louis, M.; Boudreau, D. *Anal. Methods*, **2013**, 5, 6896-6899.
8. Viger, M. L.; Brouard, D.; Boudreau, D. *J. Phys. Chem. C*, **2011**, 115, 2974-2981.
9. Asselin, J.; Roy, C.; Boudreau, D.; Messaddeq, Y.; Bouchareb, R.; Mathieu, P. *Chem. Commun.*, **2014**, 50, 13746-13749.